International Journal of Low-Carbon Technologies, 2024, **19**, 2195–2209
https://doi.org/10.1093/ijlct/ctae170
Original Article

Techno-economic and environmental analysis of an off-grid hybrid system using solar panels, wind turbine, diesel generator, and batteries for a rural health clinic considering

Tao Hai[1,2,3,4], Hayder Oleiwi Shami[5,6,*], Mohsen Ahmed[7], Diwakar Agarwal[8], Husam Rajab[9], Adil Ismaeel Mohammed[10], Abbas Hameed Abdul Hussein[11], Dheyaa Flayih Hasan[12], Hiba Mushtaq[13], Narinderjit Singh Sawaran Singh[3]

[1]School of Information and Artificial Intelligence, Nanchang Institute of Science & Technology, Nanchang 330108, China
[2] School of Computer and Information, Qiannan Normal University for Nationalities, Duyun, Guizhou, 558000, China
[3]Faculty of Data Science and Information Technology, INTI International University, 71800, Malaysia
[4]Artificial Intelligence Research Center (AIRC), Ajman University, P.O. Box 346, Ajman, UAE
[5]Department of Accounting, Al-Amarah University College, Maysan, Iraq
[6]College of Administration and Economics, Department of Economics, University of Misan, Iraq
[7]Imam Abdulrahman Bin Faisal University, P.O. Box 1982, Dammam 31441, Eastern Province, Kingdom of Saudi Arabia
[8]Department of Electronics and Communication Engineering, Institute of Engineering and Technology, GLA University, Mathura, India
[9]College of Engineering, Mechanical Engineering Department, Alasala University, King Fahad Bin Abdulaziz Rd., P.O. Box 12666 Amanah 31483, Dammam, Kingdom of Saudi Arabia
[10]Department of Anesthesia Techniques, Health and Medical Techniques College, Alnoor University, Mosul, Iraq
[11]Ahl Al Bayt University, Kerbala, Iraq
[12]College of Health and Medical Technology, National University of Science and Technology, Dhi Qar, 64001, Iraq
[13]Gilgamesh Ahliya University, Baghdad, Iraq

*Corresponding author. College of Administration and Economics, Department of Economics, University of Misan, Maysan, Iraq.
E-mail: haider.alewi@alamarahuc.edu.iq

Abstract

Middle East has significant potential for independent solar and wind power generation due to its vast land area and dispersed settlements. Enhancing the standard of living in remote areas and meeting the increasing demand for healthcare services worldwide are crucial objectives. Finding the most reliable and affordable method of supplying energy and clean water to rural healthcare institutions is the main goal of the research. The aim of this research is to evaluate the financial and environmental impacts of employing a hybrid energy system to supply power to a clinic in Rijal Almaa, Saudi Arabia. Utilizing the HOMER software, the investigation determined that the most efficient hybrid configuration includes 360 batteries, a 25 kW DG, a 2 kW wind turbine, 33.3 kW of solar panels, and an 18.4 kW converter. The NPC (Net Present Cost) associated with this optimized system amounts to $109 307, while its COE is 0.103 $/kWh. It was found that this efficient system necessitates an initial capital outlay of $72 281, coupled with an annual operational expense of $2361. The renewable fraction (RF) of 84.7%, excess electricity generation of 8.81%, and fuel consumption of 4135 L/yr are notable features of the system. The system also exhibits the lowest annual CO_2 emissions at 10825 kg/yr, indicating a positive environmental impact. The findings can be applied globally, particularly in hot, arid regions. The analysis suggests that reducing the costs of hybrid solar panels, DG, wind turbine, and battery systems could significantly reduce overall costs, making them a feasible solution for developing nations.

Keywords: renewable energy; HOMER software; techno-economic; analyzing sensitivity; optimization; hybrid energy system

1. Introduction

Remote areas lack electricity access due to high costs and technical challenges. Installing local power production plants could provide a cost-effective, reliable source of electricity in these areas [1]. Off-grid renewable energy generation in rural areas offers numerous benefits, including preventing fossil fuel depletion [2], reducing emissions, eradicating poverty, creating employment, and improving living standards [3, 4]. In the global energy market, solar power is by far the most often utilized renewable energy source [5, 6]. Saudi Arabia prioritizes sustainable electricity provision for public facilities like health clinics, enhancing social infrastructure, ensuring energy security, and transitioning towards cleaner energy sources [7].

As noted in [8], the risk of blackouts in the power grid presents a significant concern, particularly for medical facilities located in isolated rural locations that are difficult to access from the grid. Global challenges include electricity demand spikes, remote living standards, population growth, and stable power supply [9, 10]. Hybrid energy systems can address these, but also present challenges like wasted power and overproduction, necessitating effective management. [11].

Many standalone systems have traditionally used conventional electricity generation technologies like diesel generators (DGs) [12]. DGs offer cost-effective, convenient power for remote areas, but have drawbacks like frequent maintenance, inefficiency, limited diesel access, and high transportation

Received 11 June 2024; revised 30 July 2024; accepted 26 August 2024

Table 1. Various optimization tools are accessible for sizing hybrid renewable energy systems

System	Grid	Software	Location	Reference
WT/PV/DG/FC/battery	Off-Grid	HOMER	Iran	[24]
WT/PV/DG/BG/battery	Off-Grid	HOMER	Iran	[25]
Fuel cell/PV/solar collector	Stand-alone	HOMER	Australia	[26]
PV/BG/Battery	Off-grid	HOMER	India	[27]
Fuel cell/pv/biomass gasifier	Stand-alone	HOMER	India	[28]
PV/DG/battery	Stand-alone	HOMER	Bangladesh	[29]
PV/WT/battery	Stand-alone	HOMER	Iran	[30]
WT/PV/battery	Off-grid	HOMER	Iran	[31]
WT/DG/PV/battery	Off-grid	HOMER	Iran	[32]
PV/DG/FC/Electrolyzer/HT/battery	On-grid	HOMER	Saudi Arabia	[33]
PV/FC/DG/HT/Electrolyzer/battery	On-grid	HOMER	Malaysia	[34]
WT/DG/PV/battery	Stand-alone	HOMER	Syria	[35]
PV/WT/battery	Stand-alone	HOMER	China	[36]
DG/PV/battery/flywheel	Stand-alone	HOMER	Saudi Arabia	[37]

costs [13, 14]. Integrating distributed generators with renewable energy sources like solar panels is a practical solution, particularly in sunny countries [15], enhancing system dependability, reducing fossil fuel dependency, and addressing environmental issues. [16, 17]. Energy storage systems (ESSs) have proven to be beneficial in both balancing energy output and consumption and controlling the variability of sources of clean energy [18, 19]. Battery banks in ESSs store surplus energy during high generation and discharge it during peak consumption, combining DGs, solar panels, and battery banks for cost-effective, emission-minimizing electricity solutions [20]. Alongside batteries, other energy storage technologies have advanced as well, such as hydrogen tanks, flywheels, pumped storage, and supercapacitors [21]. Hydrogen storage is notable for its storage duration, density, availability, and environmental benefits [22].

Hybrid energy technologies are gaining popularity due to cost-effectiveness and efficiency. HOMER software is used for optimizing systems by evaluating power requirements and sizing components efficiently [23]. Table 1 lists several research projects that improve hybrid renewable sources using artificial intelligence and computer software.

Researchers in Saudi Arabia are using the HOMER program to optimize hybrid energy systems for a health clinic in Rijal Almaa, addressing challenges like excess electricity and grid breakeven distances.

The analysis of the literature shows how much potential there is for autonomous solar and wind power generation systems in the Kingdom of Saudi Arabia, a nation with a sizable land area and numerous scattered towns and locations. The primary objective of the research is to determine the most dependable and economical means of providing energy and clean water to rural healthcare facilities. Important goals include raising the level of living in rural areas and satisfying the growing global need for healthcare services. The research endeavors to pinpoint a cost-effective strategy for advancing rural health clinics by employing techniques for managing excess electricity, conducting sensitivity analysis, and undertaking multi-year analysis to address the aforementioned challenges.

The article examines a hybrid power system in Rijal Almaa, focusing on solar modules, a WT, DG, and battery banks for a health clinic and water desalination. The HOMER optimization tool is used to develop a long-term plan, with sensitivity analyses for general application. The findings can be applied globally, particularly in hot, arid regions.

2. Methodology

2.1. HOMER software

The investigation evaluates the technological, financial, and environmental aspects of a hybrid solar modules/WT/battery/DG system using the HOMER software. Figure 1 shows the optimization approach for hybrid systems created with HOMER software, outlining the necessary steps to reach the desired outcomes [38].

2.2. Technical analysis

2.2.1. Photovoltaic panels

Photovoltaic panels generate power when sunlight is abundant, with a diesel generator compensating for reduced output at night. The PV's capacity is maximized using the HOMER optimizer. HOMER calculates panel output using a DC bus formula [39]:

$$P_{PV} = Y_{PV} f_{PV} \left(\frac{G_T}{G_{T,STC}}\right)\left[1 + \alpha_P \left(T_C - T_{C,STC}\right)\right] \quad (1)$$

The photovoltaic array's capacity is shown as P_{PV} (kW). The derating factor is f_{PV} (%), the incident sun irradiation on the photovoltaic array is represented by G_T (W/m^2), and the incident irradiation in the typical test conditions is represented by $G_{T,\,STC}$ (W/m^2). The temperature coefficient of electricity is denoted by α_P (%/°C), the photovoltaic cell temperature is T_c (°C), and the photovoltaic cell temperature under standard circumstances is $T_{c,STC}$ (°C).

2.2.2. Diesel generator

Diesel generators are utilized as supplementary energy sources to enhance the dependability of integrated power systems [40]. DGs' performance is determined by their fuel usage and effectiveness, with HOMER incorporating a diesel generator's linear fuel curve with a y-intercept to calculate fuel consumption features.

$$F_d = \left(a.T_d + b.P_d\right) \quad (2)$$

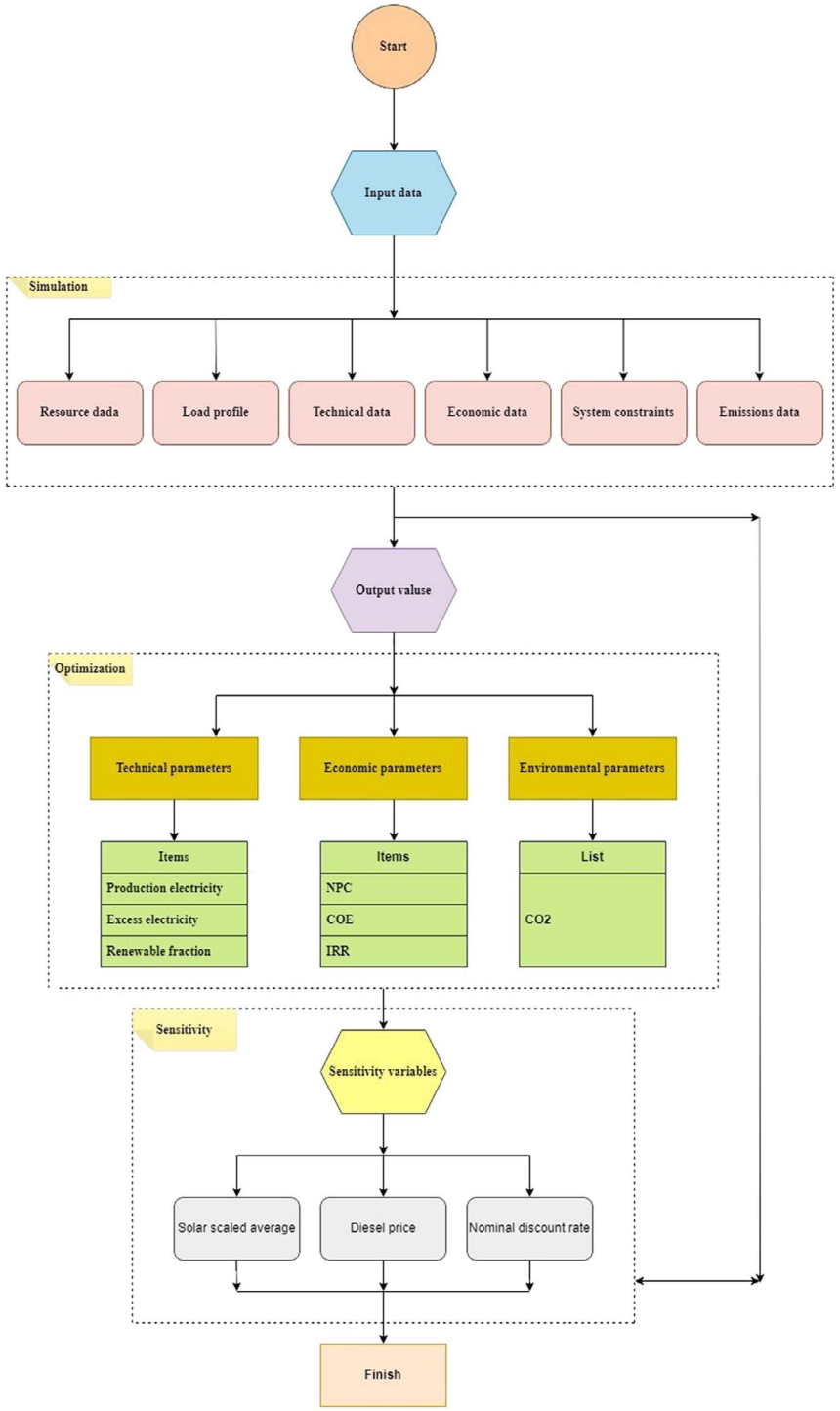

Figure 1. Hybrid system optimization flowchart.

In this context, F_d, T_d, P_d, a, and b stand for the fuel consumption rate (in liters per hour), DG capacity, DG output, fuel intercept coefficient (in liters per kilowatt-hour), and fuel slope (in liters per kilowatt-hour), respectively.

2.2.3. Battery power

To optimize the battery's strings, utilize the HOMER optimizer. Use the following equation to determine the battery system's capacity [41]:

$$C_{bat} = \frac{AD.E_l}{DOD.\eta_i.\eta_b} \quad (3)$$

where the following variables represent the load demand (kWh), depth of discharge (%), battery autonomy, battery efficiency (%), and inverter efficiency (%), respectively: E_l, DOD, AD, η_b, and η_i.

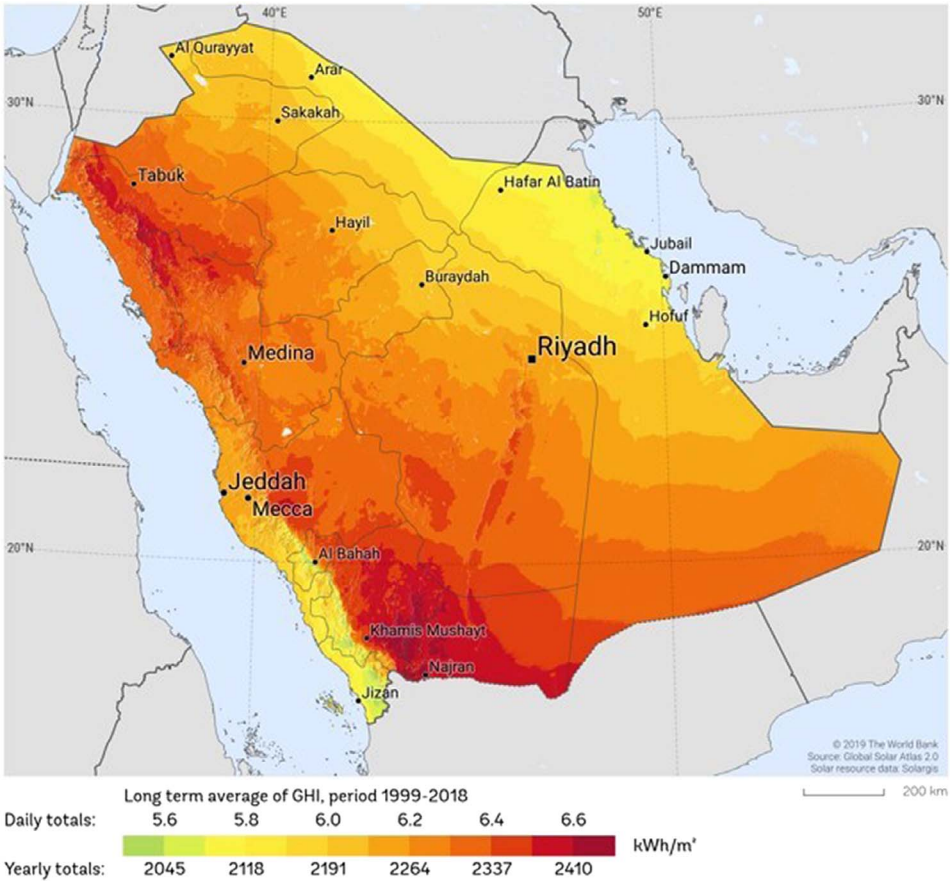

Figure 2. Average daily solar irradiation distribution in Saudi Arabia.

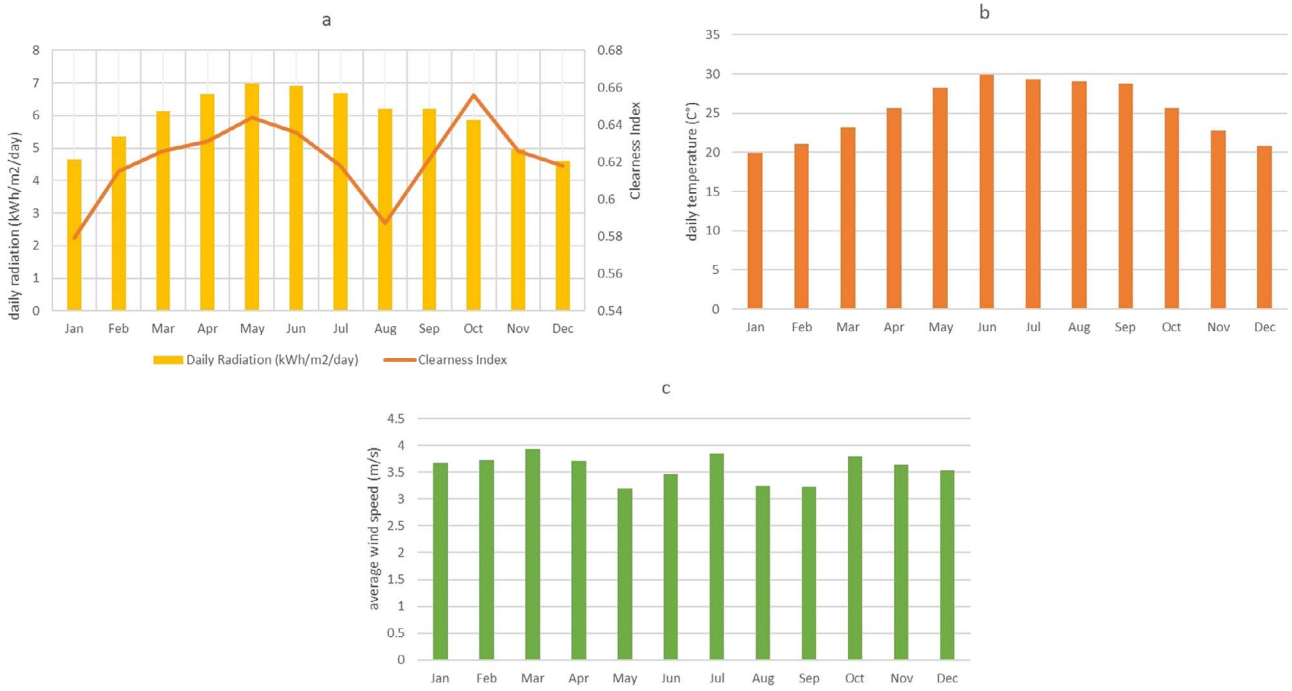

Figure 3. The monthly averages of GHI (a), temperature (b), and wind speed (c) for Rijal Almaa village.

2.2.4. Wind turbine

A wind turbine converts wind energy into electricity [42, 43]. The WT's capacity is maximized by means of the HOMER optimizer. In order to account for variations in the wind speed at various heights above the ground, HOMER calculates the wind velocity at the hub altitude [44]:

$$U_{\text{hub}} = U_{\text{anem}} \frac{\ln\left(\frac{Z_{\text{zub}}}{Z_0}\right)}{\ln\left(\frac{Z_{\text{anem}}}{Z_0}\right)} \quad (4)$$

Table 2. The breakdown of each container's energy use

Health Clinic Container			
Device	**Capacity (W)**	**Quantity ×hours**	**Energy total (kWh/d)**
Lighting	15	6 × 10	0.90
Blood/Vaccine Refrigerator	70	1 × 18	1.26
Small Refrigerator	150	1 × 24	3.60
Lab Autoclave	1500	1 × 2	3.00
Oxygen Concentrator	270	1 × 2	0.54
Suction Apparatus	100	1 × 2	0.20
Desktop Computer	150	1 × 8	1.20
Mobile Charger	20	4 × 6	0.48
Radio Receiver	32	1 × 10	0.32
Air Conditioner	400	1 × 10	4.00
Other applicants	2000	1	2.00
Total energy consumption per container			17.50
Total energy consumption for 10 containers			175

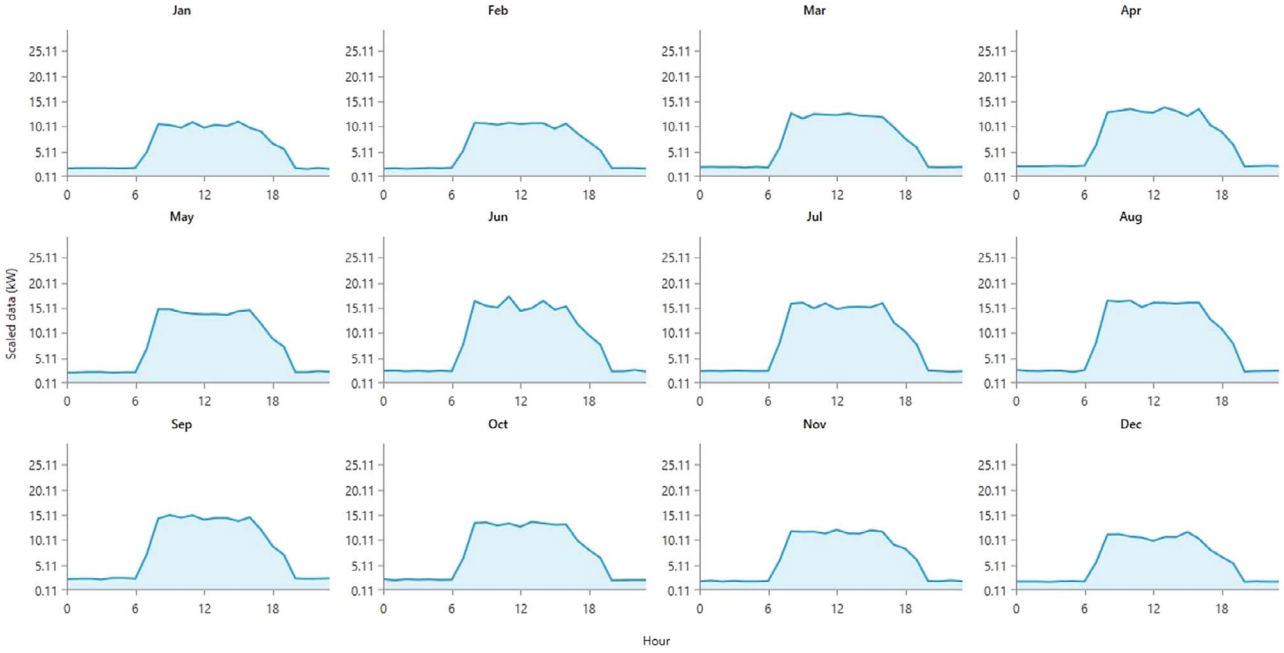

Figure 4. Daily load profile.

Parameters such as Z_{anem} (m), Z_0 (m), Z_{hub} (m), and U_{anem} (m/s) denote the hub height and anemometer height of the wind turbine, the surface roughness length, and the wind speed at anemometer height.

2.2.5. Converter

To optimize the converter's capacity, utilize the HOMER optimizer. The HOMER converter, a crucial component in hybrid energy systems, converts DC electricity into AC power using an inverter and rectifier [45]. The efficiency (ηc) of the converter is calculated by dividing the energy output (Pio) by the input energy (Pii) [46]:

$$\eta_i = \frac{P_{io}}{P_{ii}} \tag{5}$$

2.2.6. Renewable fraction

The HOMER program uses the following formula to determine the renewable fraction, or the percentage of energy produced from sustainable resources:

$$f_{ren} = 1 - \frac{E_{nonren} + H_{nonren}}{E_{served} + H_{served}} \tag{6}$$

The nonrenewable electricity and thermal production, the total electrical load served, the energy sold to the grid (included in E_{served}), the energy sold to the grid (included in E_{served}, which is zero in off-grid systems), and the total thermal load served are represented, respectively, by E_{nonren}, H_{nonren}, E_{served}, $E_{grid,\ sales}$, and H_{served} [3].

2.3. Economic analysis

2.3.1. Real discount rate

Determining the yearly real discount rate is necessary when converting single-time expenses to yearly expenses. In order to determine this rate, HOMER utilizes the equation given as [47]:

$$i = \frac{i' - f}{1 + f} \tag{7}$$

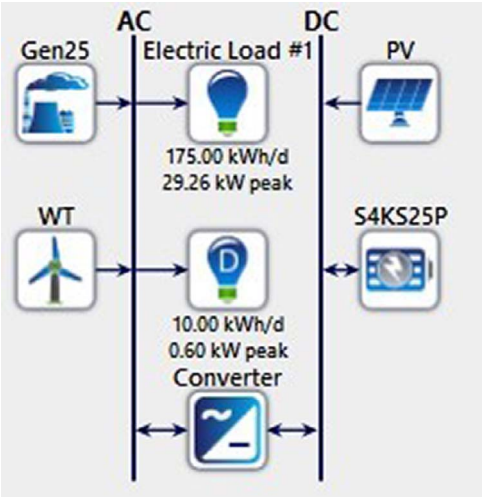

Figure 5. The setup of a hybrid battery, photovoltaic panels, WT, and DG system.

where the nominal discount rate (i'), the actual discount rate (i), and the predicted inflation rate (f) are shown.

2.3.2. NPC

NPC, or the cost of installation and system operation over a project's lifespan, is crucial for determining optimization priorities and HOMER responses, calculated using equations [48]:

$$\mathrm{NPC} = \frac{\mathrm{TAC}}{\mathrm{CRF}\,(\mathrm{i}, \mathrm{T_P})} \tag{8}$$

The formula to calculate the CRF is based on the values of TAC, T_p,i, and CRF, representing the annualized total NPC, project lifetime, real interest rate, and capital recovery factor, respectively [49]:

$$\mathrm{CRF}\,(i, n) = \frac{i(1+i)^n}{(1+\mathrm{i})^n - 1} \tag{9}$$

where n number of years.

2.3.3. Levelized cost of energy (LCOE)

The LCOE, or the mean cost of electricity produced ($/kWh) for renewable energy sources, has decreased over the last 5 years, considering various factors. [50].

$$\mathrm{COE} = \frac{C_{\mathrm{ann,tot}}}{E_{\mathrm{prim,AC}} + E_{\mathrm{prim,DC}}} \tag{10}$$

where $C_{\mathrm{ann,tot}}$, $E_{\mathrm{prim,AC}}$, and $E_{\mathrm{prim,DC}}$ stand for the total annualized cost of the primary load serviced by AC and DC (kWh/year), respectively.

2.4. Emission

Carbon dioxide is the main output gas of energy processes [51, 52]. The following formula is used to calculate CO_2 emissions in a hybrid power system [53]:

$$\mathrm{MCO_2} = 3.667\,(\mathrm{a_f H_f C_f f_c}) \tag{11}$$

Where MCO_2, the amount of gasoline (L), its value for heating (MJ/L), its carbon emission factor (ton carbon/TJ), its yearly CO_2 emissions (kg/year), and its fraction of oxidized carbon are denoted, respectively.

3. System simulation

3.1. Climate statistics

Figure 2 displays the Solar Atlas of Saudi Arabia, indicating that most parts of the country receive an average sun irradiation between 4 and 7 kWh/m^2/day, as demonstrated in the sensitivity analysis [54].

3.2. Study area

The project analyzes solar radiation conditions in Saudi Arabia, using Rijal Almaa as a sample village. Situated in the Assir Region with geographical coordinates of 18.1245° N and 42.1625° E, it serves as a link between Yemen and the Levant, with a fixed population of 2353 people and 600 families.

3.3. Wind, temperature, and solar energy data resources

The village of Rijal Almaa is described in Table 1, and the monthly averages of air temperature, wind patterns, and sun irradiation are displayed in Fig. 3(a)–(c).

3.4. Loads

The electrical requirements of a health clinic, detailing component types, quantities, operating hours, and energy usage are presented in Table 2 [55]. The maximum power usage is determined to be 17.5 kWh/day.

Health clinic containers accommodate 10 people [55], with yearly load profile estimated using HOMER software. July sees significant increase in electricity usage due to increased air conditioning use (Fig. 4).

The clinic uses a desalination device to provide freshwater for ten individuals daily, ensuring a minimum of 2.5 m^3 of water per day. About 4 kWh/m^3 are used by the reverse osmosis desalination system [56], adding 10 kWh to the daily electrical demand. The peak load for the desalination system and storage tank is 0.6 kW, which may be postponed due to off-peak periods, despite the need for energy during daylight hours. [25].

3.5. Equipment input

The hybrid power system comprises photovoltaic panels, a wind turbine, a diesel generator, batteries, converters, an AC bus, a DC bus, load demand, and additional components. Figure 5 shows the arrangement of critical components in renewable hybrid systems.

Tables 3 and 4 display component specifications and prices, while HOMER Optimizer determines the number of PV panels, converters, battery strings, and WT needed using search space.

3.6. Financial statistics

The prices of individual components can be found in Table 4. To analyze the project economically, a 25-year project lifetime, a 6% interest rate, a 2.2% inflation rate [60], and a diesel cost of 0.3067 $/L are assumed [61].

Table 3. Technical details of a hybrid battery, PV panels, wind turbine, and DG system

Component		
PV	Model	SunPower X21–335-BLK
	Type	Flat plate
	Size	335 W
	NOCT	43 °C
	Temperature coefficient	− 0.3%/°C
	Efficiency under typical test circumstances.	21%
	Derating factor (DF)	88%
	Lifetime	25 yr
Diesel generators	Model	Generic
	Size	25 kW
	Minimal ratio of load	25%
	Fuel curve's slope	0.237 L/h/kW
	Coefficient of fuel intercept	0.0825 L/h
	Lifetime	15 000 h
System converts	Model	System Converter
	Size	Auto sizing
	Efficiency of inverters	95%
	Efficiency of the rectifier	95%
	Rectifier capacity	100%
	Lifetime	15 yr
Battery	Model	Surrette 4 KS 25P
	Type	Kinetic Battery
	Nominal capacity	7.55 kWh 1890 Ah
	Round trip efficiency	80%
	Batteries per string	12
	Nominal voltage	4 V (48 V)
	Max charge current	459 A
	Minimum state of charge	40%
	Throughput	10551.7 kWh
	Lifetime	15 yr
Wind turbine	Type	AWS HC
	Size	3.3 kW
	Hub height	30 m
	Lifetime	20 yr

Table 4. Costs of system components

Component			Ref
System converts	Nominal capacity	1 kW	[57]
	Investment costs	648 $/kW	
	Replacement expenses	598 $/kW	
	Operation and maintenance expenses	5.5 $/kW/yr	
	Lifetime	15 years	
Wind turbine	Nominal capacity	3.3 kW	[30]
	Investment costs	3240 $/kW	
	Replacement costs	2268 $/kW	
	Operation and maintenance expenses	65 $/kW/yr	
	Lifetime	20 years	
Storage battery	Nominal capacity	7.55 kWh	[39]
	Investment costs	538 $/kW	
	Replacement expenses	500 $/kW	
	Maintenance and operation costs	2 $/kW/yr	
	Lifetime	15 years	
Flat plate PV	Nominal capacity	1 kW	[58]
	Investment costs	1200	
	Replacement expenses	659.6 $/kW	
	Operation and maintenance expenses	0.5 $/kW/yr	
	Lifetime	25 years	
Diesel generator	Nominal capacity	25 kW	[59]
	Investment costs	1000 $/kW	
	Replacement costs	900 $/kW	
	Maintenance and operation costs	0.02 $/kW/hr	
	Lifetime	15 000 hr	

Table 5. Settings and limits within the software that are used to regulate system operations

Items	Value
Project lifetime	25 years
Load following	Yes
Charge in cycles	Yes
Apply the set point	Yes
Set point state of charge	40%
Enabling multiple generators	Yes
Multiple generators can operate in parallel	Yes
Constraints minimal percentage of renewables	40%
Maximum yearly capacity shortage percentage	1%
Load in current time step	10%
Peak load per year	2%
Energy produced by solar panels	80%
Energy generated by wind turbines	50%

3.7. System control parameters and constraints

The module models for multiple years evolve over the project's duration, assuming 0.5% PV degradation and electric load growth annually. Fixed O&M costs are anticipated to remain steady [62]. Table 5 provides system controlling settings for simulation run limitations, including battery bank charging up to 40% capacity and predetermined charge state.

4. Results and discussion

4.1. Optimization results

Table 6 shows the village's optimization techniques. The most cost-effective power systems also had the lowest NPC and COE. The most efficient configuration was found to consist of 33.3 kW of solar modules, 2 kW of wind turbine, 25 kW of diesel generator, 360 batteries (30 strings), and 18.4 kW of converter. When the LF method was used, this system showed a low NPC ($109 307) and COE (0.103 $/kWh). On the other hand, the photovoltaic panels and DG system that employed the LF method were found to be economically unviable because of their high NPC ($350 309) and COE (0.331 $/kWh) that resulted from higher fuel, O&M, and capital costs.

The proposed WT/PV/DG/battery hybrid system, which includes PV panels, wind turbine, DG, and battery, is the least expensive and emits the fewest carbon emissions. Its initial investment cost is $72 281, with an annual running cost of $2361, an efficiency ratio of 84.7%, and fuel usage of 4135 L/yr.

4.2. Electrical outputs

Table 7 displays the power output of the ideal WT/PV/DG/Battery system, with photovoltaic power generation accounting for 77.1% of the total annual energy generated. The hybrid system uses diesel and wind power for energy, generating 12.7% and 10.2%, respectively, resulting in an 8.81% surplus of electricity.

Figure 6 shows optimal WT/PV/DG/Battery system electric generation peaks in October and March due to increased solar radiation, while January experiences a decrease due to less sun exposure.

4.3. Economic analysis

Figure 7 shows the costs of an ideal photovoltaic panels, wind turbine, DG, and battery hybrid system, highlighting high initial capital and operating costs.

The optimal photovoltaic panels, wind turbine, DG, and battery hybrid system outperformed the standard system, indicating a more economically feasible choice for cost recovery and savings throughout the project's 25-year lifespan (Fig. 8(a) and (b)).

Figure 9 shows the proposed system, which combines solar panels, wind turbines, DG, and batteries for maximum efficiency, with a projected 8.7-year payback period.

4.4. Environmental performance analysis

Table 8 shows CO_2 emissions ranking first, with PV panels, WT, DG, and battery hybrid systems being the cleanest options. However, because the PV/DG system emits the highest CO_2 (42 538 kg/yr), it appears to be the most polluting.

4.5. Sensitivity analysis

Sensitivity analysis examines how input parameter changes or uncertainty impact system behavior, requiring adjustments to factors like diesel fuel price, PV power average, and nominal discount rate. A comprehensive summary of the input variables that significantly affect the system may be found in Table 9.

Figure 10 shows COE and NPC values influenced by gasoline prices and discount rates, indicating the optimal battery hybrid system with PV panels, wind turbine, and DG. The net present value decreases and the COE increases with a 7% nominal discount rate, indicating the necessity of selecting a suitable rate for financial sustainability.

Figure 11 shows changes in NPC and COE values based on irradiation and diesel prices. As irradiation increases, both values drop, indicating that higher diesel prices directly affect energy costs in hybrid systems.

Figure 12 demonstrates that an increase in annual mean irradiation leads to a rise in renewable components and a decrease in fuel use.

Figure 13 illustrates that a rise in scaled yearly average irradiation is correlated with a decrease in CO_2 emissions. As Fig. 13 shows, there is a rise in COE and a fall in CO_2 emissions with rising diesel costs.

Figure 14 shows that scaled annual average parameters directly affect excess energy levels, with increased irradiation resulting in higher excess electricity percentage and decreased COE, and higher gasoline prices causing increased excess electricity percentage.

4.6. Policy implications

The potential of a hybrid renewable energy system using PV power in rural areas like Rijal Almaa Heritage Village in Saudi Arabia is promising. With proper investment and government support, these systems could provide a sustainable, clean solution for rural electrification. Future research should explore control strategies and hybrid energy systems blending biomass power generation.

5. Conclusion

The study assesses a hybrid power system for a rural (Rijal Almaa village) health center using the HOMER optimization

Table 6. The techno-economic attributes of the hybrid system

System	PV (kW)	WT (kW)	DG (kW)	Battery (kWh)	Converter (kW)	Dispatch	COE ($/kWh)	NPC ($)	RF (%)	Fuel (L/yr)	Excess electricity (%)	CO_2 (kg/yr)
WT/PV/DG/battery	33.31	2	25	24	18.38	LF	0.103	109 307	84.7	4135	8.81	10 825
DG/PV/battery	38.53		25	24	19.07	LF	0.105	111 561	82.9	4627	10.51	12 112
DG/WT/battery		9	25	12	9.41	CC	0.123	130 362	40.17	13 553	9.42	35 479
DG/WT/PV	13.14	24	25		6.20	LF	0.207	219 132	40.04	16 051	58.82	42 020
DG/WT		32	25			LF	0.218	231 246	40.08	15 557	60.98	40 727
DG/PV	197.6		25		25.31	LF	0.331	350 389	40.02	16 249	83.07	42 538

Table 7. Electricity generation and usage for optimal PV/WT/DG/battery setup

Component	Production (kWh/yr)	Percent
SunPower X21–335-BLK Generic 25 kW Fixed Capacity Genset	62 577 10 336	77.1 12.7
AWS HC 3.3 kW Wind Turbine	8287	10.2
Total	81 200	100
Component	Consumption (kWh/yr)	Percent
AC primary load	63 875	94.6
DC primary load	0	0
Deferrable load	3649	5.4
Total	67 524	100
Quantity	Value	Units
Excess electricity	7151	kWh/yr
Unmet electric load	0	kWh/yr
Capacity shortage	1.03	kWh/yr

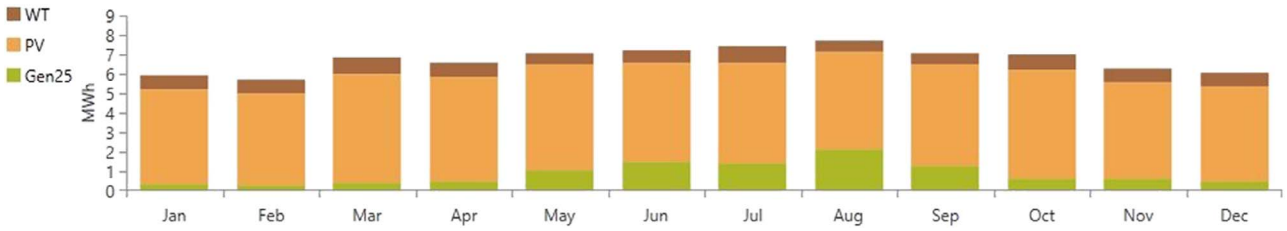

Figure 6. The average monthly output of power for the most effective WT/PV/DG/Battery configuration.

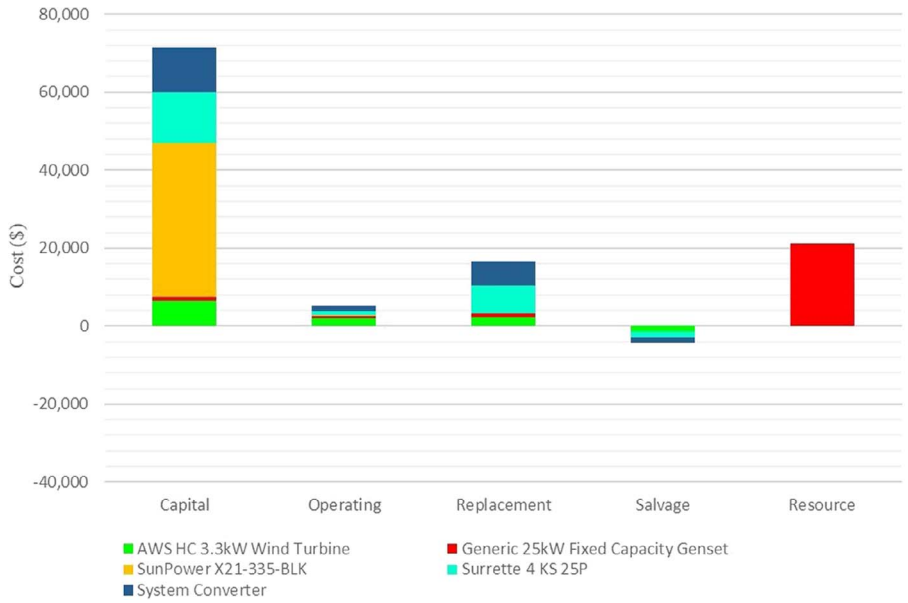

Figure 7. Summarizes the NPC of the optimal PV/DG/WT/battery hybrid configuration.

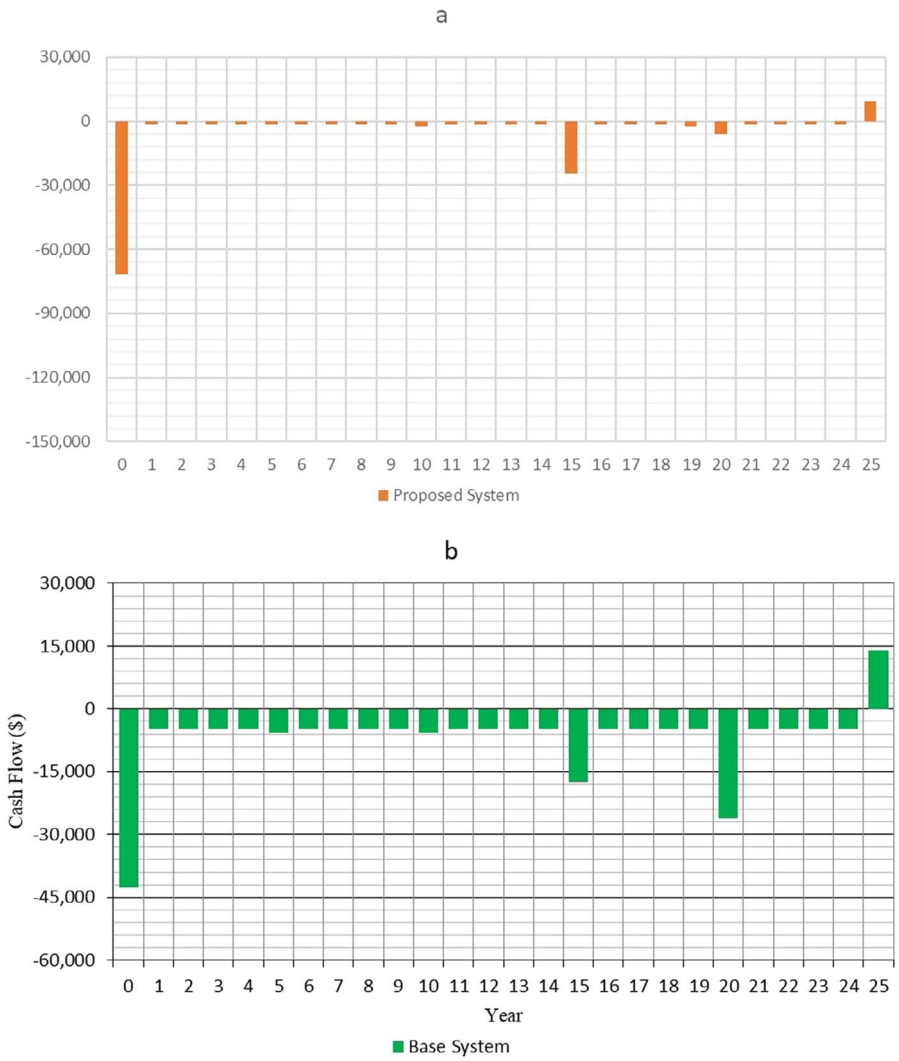

Figure 8. Compares the yearly nominal cash flow differences between the most efficient (a) and base systems (b).

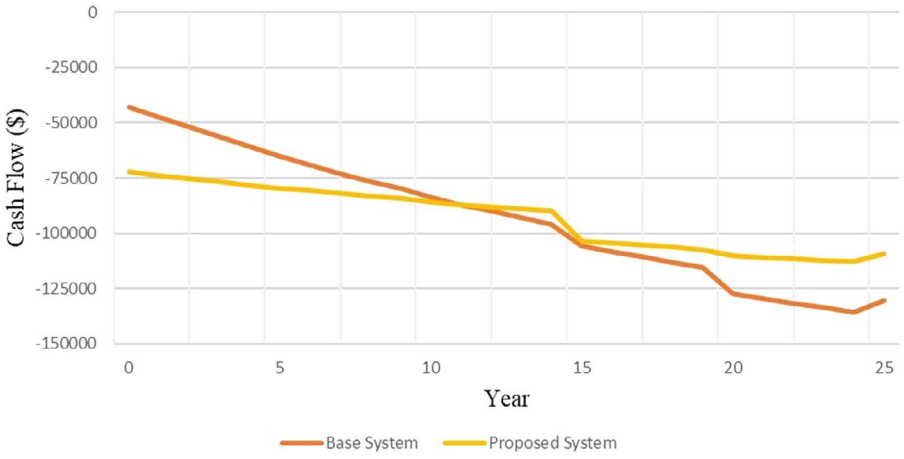

Figure 9. A breakdown of the total cash flow in relation to the suggested system and the original system.

tool, analyzing environmental, technological, and economic aspects. It evaluates the long-term viability using NPC and COE metrics, sensitivity analyses, and input variables. In brief, the primary findings of this research are delineated as follows:

- The PV/WT/DG/battery configuration is the most economically advantageous hybrid system. The LF strategy results in the lowest NPC ($109 307) and COE (0.103 $/kWh) for this system, making it the most environmentally friendly with CO_2 emissions of 10 825 kg/yr.

Table 8. Emissions are released from every conceivable system

Pollutant	Quantity (kg/yr)
CO_2	11 229
CO	70.1
UHC	3.09
PM	0.420
SO_2	27.5
NO_2	65.9

Table 9. The ideal system parameters' sensitivity analysis variables span a broad range

Sensitivity parameters	Unit	Ranges
Nominal discount rate	%	6–7, intervals 0.25
Solar scaled average	kWh/m^2/day	5.93–6.21, intervals 0.2
Gasoline cost	$/L	0.3067–0.3867, intervals 0.2

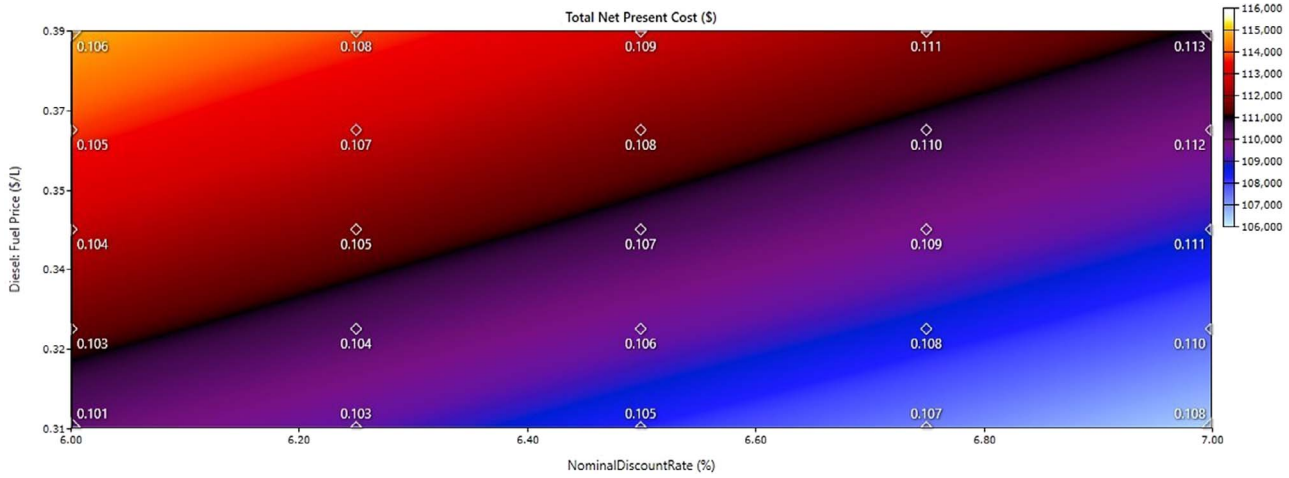

Figure 10. The effects of changing the Diesel price and nominal discount % on the system's NPC and COE.

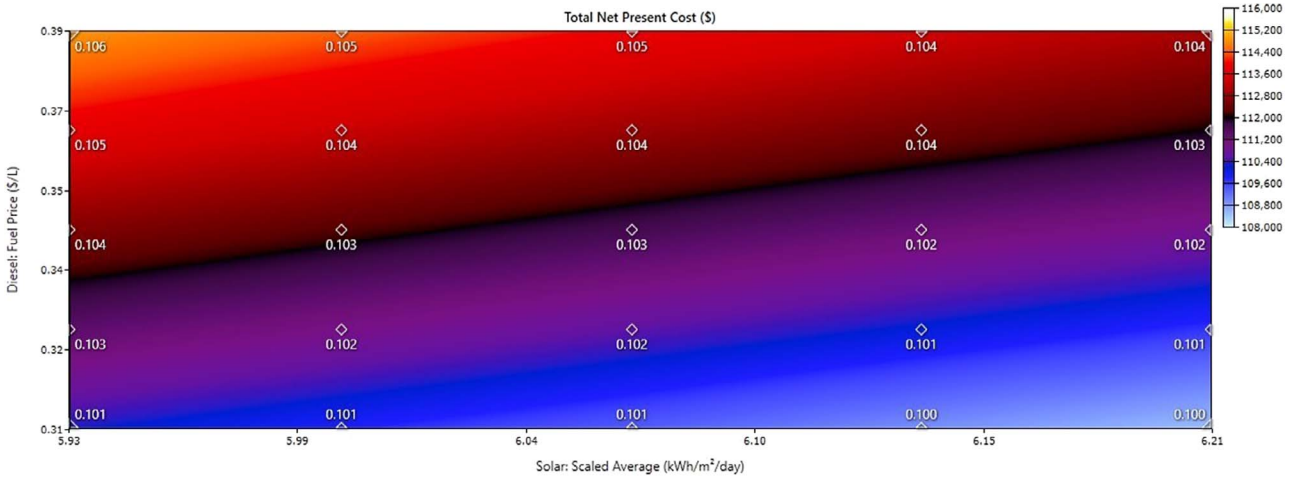

Figure 11. The effects of scaled yearly average radiation and variations in diesel prices on the system's NPC and COE.

Conversely, the PV/DG system employing the LF strategy is deemed economically unfeasible due to its notably high NPC of $350 309 and COE of 0.331$/kWh. The system's high initial cost, high energy costs, and high CO_2 emissions due to the absence of PV panels and wind turbines contribute to its high initial cost.

- The most efficient PV/WT/DG/battery system uses PV power for 77.1% of total electricity production, with

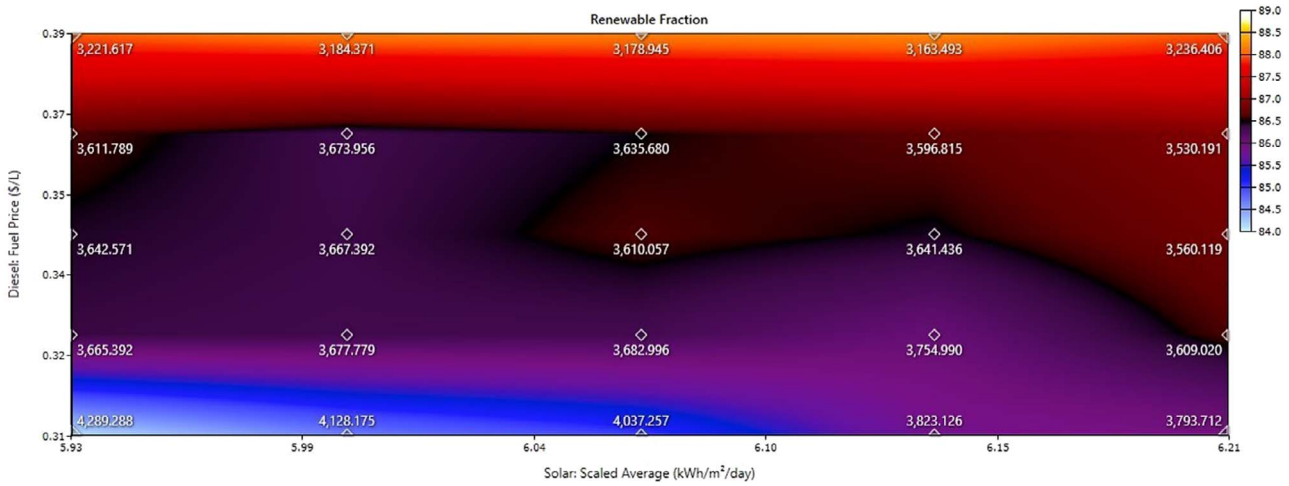

Figure 12. The effects of changes in diesel prices and scaled yearly average radiation on fuel consumption and the renewable proportion.

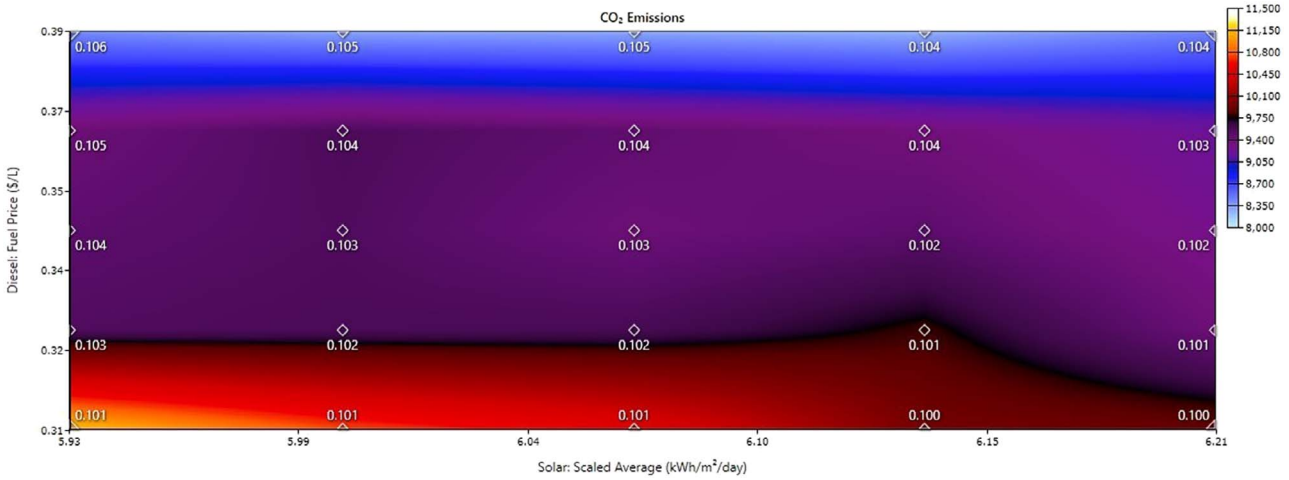

Figure 13. The effects of scaled yearly average irradiance and variations in diesel price on CO_2 emissions and COE.

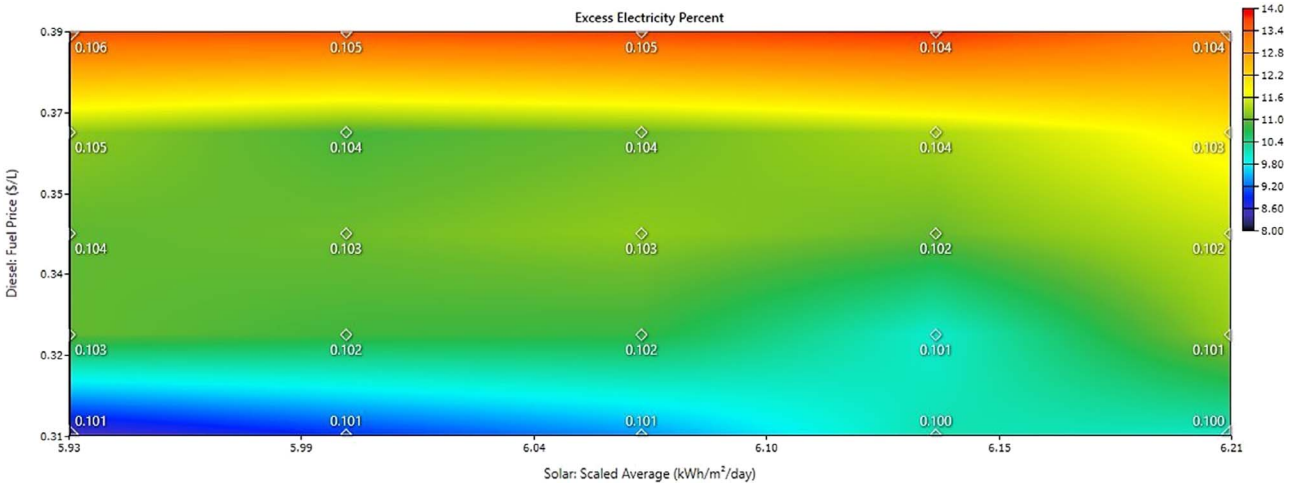

Figure 14. The changes in diesel price and scaled annual average irradiation on excess electricity percentage and COE.

diesel and wind power for 12.7% and 10.2%, respectively. The system generates an excess of 7151 kWh/yr (8.81%) annually.

- The optimal nominal discount rate, ranging from 6% to 7%, significantly impacts the system's NPC value, highlighting the importance of selecting the right rate. Furthermore, when diesel fuel prices climb from 0.3067 $/L to 0.3867 $/L, the COE and NPC values of the ideal system increase, indicating that high diesel costs negatively impact the financial elements of DG-based hybrid systems.

Overall, the primary findings of the techno-economic optimization indicate that the hybrid PV/WT/DG/battery is the best choice for a rural health center in Rijal Almaa village.

Acknowledgements

This work is supported by the science and technology foundation of Guizhou Province No. ZK[2024]661.

Author contributions

Tao Hai (Data curation [equal], Investigation [equal], Validation [equal]), Hayder Shami (Methodology [equal], Project administration [equal], Writing—original draft [equal]), Mohsen Ahmed (Formal analysis [equal], Investigation [equal], Writing—review & editing [equal]), Diwakar Agarwal (Methodology [equal], Validation [equal], Writing—review & editing [equal]), Husam Rajab (Data curation [equal], Formal analysis [equal], Validation [equal]), Adil Mohammed (Formal analysis [equal], Writing—original draft [equal]), Abbas Abdul Hussein (Conceptualization [equal], Data curation [equal], Formal analysis [equal], Writing—review & editing [equal]), Dheyaa Hasan (Formal analysis [equal], Investigation [equal], Methodology [equal]), Hiba Mushtaq (Resources [equal], Software [equal], Writing—review & editing [equal]), Narinderjit Sawaran Singh (Formal analysis [equal], Investigation [equal], Methodology [equal], Writing—original draft [equal]).

Funding

None declared.

References

1. Das M, Singh MAK, Biswas A. Techno-economic optimization of an off-grid hybrid renewable energy system using metaheuristic optimization approaches–case of a radio transmitter station in India. *Energy Convers Manag* 2019;**185**:339–52. https://doi.org/10.1016/j.enconman.2019.01.107.
2. Meng Q, Jin X, Luo F. *et al.* Distributionally robust scheduling for benefit allocation in regional integrated energy system with multiple stakeholders. *J Mod Power Syst Clean Energy* 2024;1–12. https://doi.org/10.35833/MPCE.2023.000661.
3. Elkadeem MR, Wang S, Sharshir SW. *et al.* Feasibility analysis and techno-economic design of grid-isolated hybrid renewable energy system for electrification of agriculture and irrigation area: a case study in Dongola, Sudan. *Energy Convers Manag* 2019;**196**:1453–78. https://doi.org/10.1016/j.enconman.2019.06.085.
4. Xu H, Yang C, Li X. *et al.* How do fintech, digitalization, green technologies influence sustainable environment in CIVETS nations? An evidence from CUP FM and CUP BC approaches. *Resour Policy* 2024;**92**:104994. https://doi.org/10.1016/j.resourpol.2024.104994.
5. Sulaiman, Alsagri A. Design and dynamic simulation of a photovoltaic thermal-organic Rankine cycle considering heat transfer between components. *Energy Convers Manag* 2020;**225**:113435. https://doi.org/10.1016/j.enconman.2020.113435.
6. Zhu C, Wang M, Guo M. *et al.* Optimizing solar-driven multigeneration systems: a cascade heat recovery approach for power, cooling, and freshwater production. *Appl Therm Eng* 2024;**240**:122214. https://doi.org/10.1016/j.applthermaleng.2023.122214.
7. Shaahid SM, El-Amin. Techno-economic evaluation of off-grid hybrid photovoltaic–diesel–battery power systems for rural electrification in Saudi Arabia—a way forward for sustainable development. *Renew Sust Energ Rev* 2009;**13**:625–33. https://doi.org/10.1016/j.rser.2007.11.017.
8. Bukar AL, Tan CW, Yiew LK. *et al.* A rule-based energy management scheme for long-term optimal capacity planning of grid-independent microgrid optimized by multi-objective grasshopper optimization algorithm. *Energy Convers Manag* 2020;**221**:113161. https://doi.org/10.1016/j.enconman.2020.113161.
9. Duan Y, Zhao Y, Hu J. An initialization-free distributed algorithm for dynamic economic dispatch problems in microgrid: modeling, optimization and analysis. *Sustain Energy Grids Netw* 2023;**34**:101004. https://doi.org/10.1016/j.segan.2023.101004.
10. Shirkhani M, Tavoosi J, Danyali S. *et al.* A review on microgrid decentralized energy/voltage control structures and methods. *Energy Rep* 2023;**10**:368–80. https://doi.org/10.1016/j.egyr.2023.06.022.
11. Akhtari MR, Baneshi M. Techno-economic assessment and optimization of a hybrid renewable co-supply of electricity, heat and hydrogen system to enhance performance by recovering excess electricity for a large energy consumer. *Energy Convers Manag* 2019;**188**:131–41. https://doi.org/10.1016/j.enconman.2019.03.067.
12. Mandal S, Das BK, Hoque N. Optimum sizing of a stand-alone hybrid energy system for rural electrification in Bangladesh. *J Clean Prod* 2018;**200**:12–27. https://doi.org/10.1016/j.jclepro.2018.07.257.
13. Zhu Y, Tong Q, Yan X. *et al.* Optimal design of multi-energy complementary power generation system considering fossil energy scarcity coefficient under uncertainty. *J Clean Prod* 2020;**274**:122732. https://doi.org/10.1016/j.jclepro.2020.122732.
14. Zhu C, Zhang Y, Wang M. *et al.* Optimization, validation and analyses of a hybrid PV-battery-diesel power system using enhanced electromagnetic field optimization algorithm and ε-constraint. *Energy Rep* 2024;**11**:5335–49. https://doi.org/10.1016/j.egyr.2024.04.043.
15. Li B, Wang J, Nassani AA. *et al.* The future of green energy: a panel study on the role of renewable resources in the transition to a green economy. *Energy Econ* 2023;**127**:107026. https://doi.org/10.1016/j.eneco.2023.107026.
16. Ashraf MA, Liu Z, Alizadeh A. *et al.* Designing an optimized configuration for a hybrid PV/diesel/battery energy system based on metaheuristics: a case study on Gobi Desert. *J Clean Prod* 2020;**270**:122467. https://doi.org/10.1016/j.jclepro.2020.122467.
17. Zheng C, Chen H. Revisiting the linkage between financial inclusion and energy productivity: technology implications for climate change. *Sustain Energy Technol Assess* 2023;**57**:103275. https://doi.org/10.1016/j.seta.2023.103275.
18. Shang C, Srinivasan D, Reindl T. Generation-scheduling-coupled battery sizing of stand-alone hybrid power systems. *Energy* 2016;**114**:671–82. https://doi.org/10.1016/j.energy.2016.07.123.
19. Wang R, Zhang R. Techno-economic analysis and optimization of hybrid energy systems based on hydrogen storage for sustainable energy utilization by a biological-inspired optimization algorithm. *J Energy Storage* 2023;**66**:107469. https://doi.org/10.1016/j.est.2023.107469.
20. Cai W, Li X, Maleki A. *et al.* Optimal sizing and location based on economic parameters for an off-grid application of a hybrid system with photovoltaic, battery and diesel technology. *Energy* 2020;**201**:117480. https://doi.org/10.1016/j.energy.2020.117480.
21. Muh E, Tabet F. Comparative analysis of hybrid renewable energy systems for off-grid applications in southern Cameroons. *Renew Energy* 2019;**135**:41–54. https://doi.org/10.1016/j.renene.2018.11.105.
22. Luta DN, Raji AK. Decision-making between a grid extension and a rural renewable off-grid system with hydrogen generation. *Int J Hydrog Energy* 2018;**43**:9535–48. https://doi.org/10.1016/j.ijhydene.2018.04.032.
23. Cuesta MA, Castillo-Calzadilla T, Borges CE. A critical analysis on hybrid renewable energy modeling tools: an emerging opportunity to include social indicators to optimise systems in small communities. *Renew Sust Energ Rev* 2020;**122**:109691. https://doi.org/10.1016/j.rser.2019.109691.
24. Razmjoo A, Gakenia Kaigutha L, Vaziri Rad MA. *et al.* A technical analysis investigating energy sustainability utilizing reliable renewable energy sources to reduce CO^2 emissions in a high potential area. *Renew Energy* 2021;**164**:46–57. https://doi.org/10.1016/j.renene.2020.09.042.
25. Rad MAV, Shahsavari A, Rajaee F. *et al.* Techno-economic assessment of a hybrid system for energy supply in the affected

areas by natural disasters: a case study. *Energy Convers Manag* 2020;**221**:113170.
26. Assaf J, Shabani B. A novel hybrid renewable solar energy solution for continuous heat and power supply to standalone-alone applications with ultimate reliability and cost effectiveness. *Renew Energy* 2019;**138**:509–20. https://doi.org/10.1016/j.renene.2019.01.099.
27. Kobayakawa T, Kandpal TC. Optimal resource integration in a decentralized renewable energy system: assessment of the existing system and simulation for its expansion. *Energy Sustain Dev* 2016;**34**:20–9. https://doi.org/10.1016/j.esd.2016.06.006.
28. Singh A, Baredar P. Techno-economic assessment of a solar PV, fuel cell, and biomass gasifier hybrid energy system. *Energy Rep* 2016;**2**:254–60. https://doi.org/10.1016/j.egyr.2016.10.001.
29. Das BK, Zaman F. Performance analysis of a PV/diesel hybrid system for a remote area in Bangladesh: effects of dispatch strategies, batteries, and generator selection. *Energy* 2019;**169**:263–76. https://doi.org/10.1016/j.energy.2018.12.014.
30. Ghorbani N, Kasaeian A, Toopshekan A. *et al.* Optimizing a hybrid wind-PV-battery system using GA-PSO and MOPSO for reducing cost and increasing reliability. *Energy* 2018;**154**:581–91. https://doi.org/10.1016/j.energy.2017.12.057.
31. Mohammadi M, Ghasempour R, Razi Astaraei F. *et al.* Optimal planning of renewable energy resource for a residential house considering economic and reliability criteria. *Int J Electr Power Energy Syst* 2018;**96**:261–73. https://doi.org/10.1016/j.ijepes.2017.10.017.
32. Jahangir MH, Mousavi SA, Vaziri Rad MA. A techno-economic comparison of a photovoltaic/thermal organic Rankine cycle with several renewable hybrid systems for a residential area in Rayen, Iran. *Energy Convers Manag* 2019;**195**:244–61. https://doi.org/10.1016/j.enconman.2019.05.010.
33. Alsagri AS, Alrobaian AA, Nejlaoui M. Techno-economic evaluation of an off-grid health clinic considering the current and future energy challenges: a rural case study. *Renew Energy* 2021;**169**:34–52. https://doi.org/10.1016/j.renene.2021.01.017.
34. Isa NM, Das HS, Tan CW. *et al.* A techno-economic assessment of a combined heat and power photovoltaic/fuel cell/battery energy system in Malaysia hospital. *Energy* 2016;**112**:75–90. https://doi.org/10.1016/j.energy.2016.06.056.
35. Merei G, Berger C, Sauer DU. Optimization of an off-grid hybrid PV–wind–diesel system with different battery technologies using genetic algorithm. *Sol Energy* 2013;**97**:460–73. https://doi.org/10.1016/j.solener.2013.08.016.
36. He L, Zhang S, Chen Y. *et al.* Techno-economic potential of a renewable energy-based microgrid system for a sustainable large-scale residential community in Beijing, China. *Renew Sust Energ Rev* 2018;**93**:631–41. https://doi.org/10.1016/j.rser.2018.05.053.
37. Ramli MA, Hiendro A, Twaha S. Economic analysis of PV/diesel hybrid system with flywheel energy storage. *Renew Energy* 2015;**78**:398–405. https://doi.org/10.1016/j.renene.2015.01.026.
38. Bahramara S, Moghaddam MP, Haghifam MR. Optimal planning of hybrid renewable energy systems using HOMER: a review. *Renew Sust Energ Rev* 2016;**62**:609–20. https://doi.org/10.1016/j.rser.2016.05.039.
39. Aziz AS, Tajuddin MFN, Adzman MR. *et al.* Feasibility analysis of grid-connected and islanded operation of a solar PV microgrid system: a case study of Iraq. *Energy* 2020;**191**:116591. https://doi.org/10.1016/j.energy.2019.116591.
40. Bajpai P, Dash V. Hybrid renewable energy systems for power generation in stand-alone applications: a review. *Renew Sust Energ Rev* 2012;**16**:2926–39. https://doi.org/10.1016/j.rser.2012.02.009.
41. Ramli MAM, Bouchekara HREH, Alghamdi AS. Optimal sizing of PV/wind/diesel hybrid microgrid system using multi-objective self-adaptive differential evolution algorithm. *Renew Energy* 2018;**121**:400–11. https://doi.org/10.1016/j.renene.2018.01.058.
42. Zhao D, Wang H, Cui L. Frequency-chirprate synchrosqueezing-based scaling chirplet transform for wind turbine nonstationary fault feature time–frequency representation. *Mech Syst Signal Process* 2024;**209**:111112. https://doi.org/10.1016/j.ymssp.2024.111112.
43. Zhu D, Wang Z, Hu J. *et al.* Rethinking fault ride-through control of DFIG-based wind turbines from new perspective of rotor-port impedance characteristics. *IEEE Trans Sustain Energy* 2024;**15**:2050–62. https://doi.org/10.1109/TSTE.2024.3395985.
44. Gualtieri G, Secci S. Methods to extrapolate wind resource to the turbine hub height based on power law: a 1-h wind speed vs. Weibull distribution extrapolation comparison. *Renew Energy* 2012;**43**:183–200. https://doi.org/10.1016/j.renene.2011.12.022.
45. El-houari H, Allouhi A, Salameh T. *et al.* Energy, economic, environment (3E) analysis of WT-PV-battery autonomous hybrid power plants in climatically varying regions. *Sustain Energy Technol Assess* 2021;**43**:100961. https://doi.org/10.1016/j.seta.2020.100961.
46. Mousavi SA, Zarchi RA, Astaraei FR. *et al.* Decision-making between renewable energy configurations and grid extension to simultaneously supply electrical power and fresh water in remote villages for five different climate zones. *J Clean Prod* 2021;**279**:123617. https://doi.org/10.1016/j.jclepro.2020.123617.
47. Ngan MS, Tan CW. Assessment of economic viability for PV/wind/diesel hybrid energy system in southern peninsular Malaysia. *Renew Sust Energ Rev* 2012;**16**:634–47. https://doi.org/10.1016/j.rser.2011.08.028.
48. Ibrahim MM, Mostafa NH, Osman AH. *et al.* Performance analysis of a stand-alone hybrid energy system for desalination unit in Egypt. *Energy Convers Manag* 2020;**215**:112941. https://doi.org/10.1016/j.enconman.2020.112941.
49. Arévalo P, Benavides D, Lata-García J. *et al.* Energy control and size optimization of a hybrid system (photovoltaic-hidrokinetic) using various storage technologies. *Sustain Cities Soc* 2020;**52**:101773. https://doi.org/10.1016/j.scs.2019.101773.
50. Grossmann WD, Grossmann I, Steininger KW. Distributed solar electricity generation across large geographic areas, part I: a method to optimize site selection, generation and storage. *Renew Sust Energ Rev* 2013;**25**:831–43. https://doi.org/10.1016/j.rser.2012.08.018.
51. Zhu C, Wang M, Guo M. *et al.* An innovative process design and multi-criteria study/optimization of a biomass digestion-supercritical carbon dioxide scenario toward boosting a geothermal-driven cogeneration system for power and heat. *Energy* 2024;**292**:130408. https://doi.org/10.1016/j.energy.2024.130408.
52. Zhu C, Zhang Y, Wang M. *et al.* Simulation and comprehensive study of a new trigeneration process combined with a gas turbine cycle, involving transcritical and supercritical CO_2 power cycles and Goswami cycle. *J Therm Anal Calorim* 2024;**149**:6361–84. https://doi.org/10.1007/s10973-024-13182-9.
53. Haffaf A, Lakdja F, Meziane R. *et al.* Study of economic and sustainable energy supply for water irrigation system (WIS). *Sustain Energy Grids Netw* 2021;**25**:100412. https://doi.org/10.1016/j.segan.2020.100412.
54. Solar resource maps of Saudi Arabia. https: //solargis.com/maps-and-gis-data/download/saudi-arabia (10 April 2024, date last accessed).
55. Olatomiwa L, Blanchard R, Mekhilef S. *et al.* Hybrid renewable energy supply for rural healthcare facilities: an approach to quality healthcare delivery. *Sustain Energy Technol Assess* 2018;**30**:121–38. https://doi.org/10.1016/j.seta.2018.09.007.
56. Peng W, Maleki A, Rosen MA. *et al.* Optimization of a hybrid system for solar-wind-based water desalination by reverse osmosis: comparison of approaches. *Desalination* 2018;**442**:16–31. https://doi.org/10.1016/j.desal.2018.03.021.
57. Mekonnen T, Bhandari R, Ramayya V. Modeling, analysis and optimization of grid-integrated and islanded solar PV Systems for the Ethiopian Residential Sector: considering an emerging utility tariff plan for 2021 and beyond. *Energies* 2021;**14**:3360. https://doi.org/10.3390/en14113360.
58. Singh S, Singh M, Kaushik SC. Feasibility study of an islanded microgrid in rural area consisting of PV, wind, biomass and battery

energy storage system. *Energy Convers Manag* 2016;**128**:178–90. https://doi.org/10.1016/j.enconman.2016.09.046.
59. Ali L, Shahnia F. Determination of an economically-suitable and sustainable standalone power system for an off-grid town in Western Australia. *Renew Energy* 2017;**106**:243–54. https://doi.org/10.1016/j.renene.2016.12.088.
60. Saudi Central Bank. 2024. https://www.sama.gov.sa/en-US/pages/default.aspx (12 April 2024, date last accessed).
61. Saudi Arabia diesel prices. *GlobalPetrolPrices.com*. https://www.globalpetrolprices.com/Saudi-Arabia/diesel_prices/ (12 April 2024, date last accessed).
62. Aziz AS, Tajuddin MFN, Adzman MR. *et al*. Optimization and sensitivity analysis of standalone hybrid energy systems for rural electrification: a case study of Iraq. *Renew Energy* 2019;**138**:775–92. https://doi.org/10.1016/j.renene.2019.02.004.